

Anomalous Dynamics and Equilibration in the Classical Heisenberg Chain

Adam J. McRoberts,¹ Thomas Bilitewski,^{1,2,3} Masudul Haque,^{1,4,5} and Roderich Moessner¹

¹Max Planck Institute for the Physics of Complex Systems, Nöthnitzer Str. 38, 01187 Dresden, Germany

²JILA, NIST, and Department of Physics, University of Colorado, Boulder, CO 80309, USA

³Center for Theory of Quantum Matter, University of Colorado, Boulder, CO 80309, USA

⁴Department of Theoretical Physics, Maynooth University, Co. Kildare, Ireland

⁵Institut für Theoretische Physik, Technische Universität Dresden, 01062 Dresden, Germany

(Dated: August 30, 2021)

The search for departures from standard hydrodynamics in many-body systems has yielded a number of promising leads, especially in low dimension. Here we study one of the simplest classical interacting lattice models, the nearest-neighbour Heisenberg chain, with temperature as tuning parameter. Our numerics expose strikingly different spin dynamics between the antiferromagnet, where it is largely diffusive, and the ferromagnet, where we observe strong evidence either of spin superdiffusion or an extremely slow crossover to diffusion. This difference also governs the equilibration after a quench, and, remarkably, is apparent even at very high temperatures.

Introduction.—Hydrodynamics has long been a cornerstone of our understanding of many-body systems, and has recently become the focus of renewed inquiry. Phenomena of interest in low-dimensional quantum systems include equilibration [1, 2], anomalous diffusion and transport [3–12], fracton and dipole-moment conserving hydrodynamics [13–15], generalised hydrodynamics in integrable quantum systems [16–28], and weak integrability breaking [29, 30]. Hydrodynamics in classical many-body systems in low dimensions also poses many questions, perhaps most notably the appearance of anomalous diffusion and anomalous transport, often attributed to the Kardar-Parisi-Zhang (KPZ) universality class [31–46].

The focus of this work is the classical Heisenberg spin chain, for which the nature of hydrodynamics has provoked extensive debate. Based on the lack of integrability, it has been argued that ordinary diffusion holds for both spin and energy [47–53]. However, there have also been proposals of anomalous behaviour [54–57], including an argument for logarithmically enhanced diffusion [57], based on the emergence of the linear momentum from the continuum limit as a hydrodynamic mode. Ref. [53], in contrast, has argued from a theory of non-abelian hydrodynamics that each component of the spin follows a separate, ordinary diffusion equation.

In this paper, we present a systematic numerical study of the dynamical correlations and equilibration dynamics over a wide range of temperatures, $T < |J|$ to $T = \infty$. We provide strong numerical evidence for ordinary diffusion of both spin and energy at $T = \infty$ and ordinary diffusion of energy at all (nonzero) temperatures in both the ferromagnetic (FM) and antiferromagnetic (AFM) chains. Most strikingly, we find a qualitative difference between ferromagnetic and antiferromagnetic models at finite temperatures. This manifests as a *temperature-dependent* finite-time dynamical exponent in the spin correlations of the ferromagnetic chain, which departs from the diffusive exponent $\alpha = 1/2$ at $T = \infty$; whereas the antiferromagnetic chain displays behaviour compati-

ble with spin diffusion at all temperatures studied. Importantly, this deviation is apparent even at high temperatures, where the correlation length is still of the order of a single lattice spacing – far from the low-temperature regime where the distinction between quadratic ferromagnetic and linear antiferromagnetic spin-wave spectra may play a role. We have thus identified a, hitherto perhaps unappreciated, fundamental difference between the dynamics of the FM and AFM models. Conceptually, this suggests that microscopic details may be essential to an understanding of long length- and timescale properties.

The behaviour of the ferromagnet could be interpreted as anomalous diffusion with a temperature-dependent exponent, or alternatively as a crossover at remarkably large timescales, rendering diffusion in practice unobservable experimentally for a wide range of temperatures. Intriguingly, at low temperatures where we obtain the best fit to a single power-law, we observe almost perfect KPZ scaling across three decades in time. This suggests that claims of KPZ behaviour also merit careful examination.

As a related phenomenon, we study equilibration dynamics after quenches from an XY to a Heisenberg chain. We establish that the observed equilibrium exponents also determine the equilibration tails of observables. Equilibration is shown to proceed via a power-law approach to the equilibrium value, with an exponent determined by that observed in the corresponding unequal-time equilibrium correlation function, again displaying anomalous finite-time exponents in the case of the FM.

Model.—We consider the periodic-boundary classical Heisenberg chain, with Hamiltonian

$$\mathcal{H} = -J \sum_{i=1}^L \mathbf{S}_i \cdot \mathbf{S}_{i+1}, \quad \mathbf{S}_1 = \mathbf{S}_{L+1}, \quad (1)$$

for unit length classical spins $\mathbf{S}_i \in S^2$. Here $J = 1$ for the FM chain, and $J = -1$ for the AFM chain.

The dynamics is given by the classical Landau-Lifshitz

equation of motion,

$$\dot{\mathbf{S}}_i = \{\mathbf{S}_i, \mathcal{H}\} = J\mathbf{S}_i \times (\mathbf{S}_{i-1} + \mathbf{S}_{i+1}), \quad (2)$$

which is solved numerically either with the standard fourth-order Runge-Kutta (RK4) algorithm or, for longer simulation times, a symplectic discrete-time odd-even (DTOE) algorithm [58].

In equilibrium, we probe the spin-spin correlations

$$\mathcal{C}^S(j, t) = \langle \mathbf{S}_j(t) \cdot \mathbf{S}_0(0) \rangle, \quad (3)$$

and the energy correlations

$$\mathcal{C}^E(j, t) = \langle E_j(t)E_0(0) \rangle - \mathcal{E}^2, \quad (4)$$

where $E_j = -J\mathbf{S}_j \cdot \mathbf{S}_{j+1}$ is the bond energy, and $\mathcal{E} = \langle E \rangle$ is the internal energy density. We use internal energy and temperature interchangeably, via $\mathcal{E}(T) = T - \coth(1/T)$ [58, 59]. Also, the (equal-time) spin correlation length is

$$\xi(\mathcal{E}) = -1/\log(-\mathcal{E}), \quad (5)$$

which, as a function of \mathcal{E} , is the same for the Heisenberg (1) and XY chains (11) [58].

Both of these correlation functions are symmetric under parity and time-reversal. To evaluate these correlations for a given \mathcal{E} , we first construct an ensemble of 20,000 initial states drawn from the canonical ensemble of \mathcal{H} at the temperature $T(\mathcal{E})$ [58]. Each state is evolved in time, cf. (2), with snapshots stored at intervals of $\Delta t = 10J^{-1}$. The correlation function at a fixed time difference t is calculated by averaging over 1000 consecutive snapshots for every initial state.

Hydrodynamics and Scaling Functions.—The hydrodynamic theory posits an asymptotic scaling form for the correlations of the conserved densities,

$$\mathcal{C}(x, t) \sim t^{-\alpha} \mathcal{F}(t^{-\alpha} x), \quad (6)$$

with a scaling exponent α and universal function \mathcal{F} .

Ordinary diffusion corresponds to an exponent of $\alpha = 1/2$, and a Gaussian scaling function. Given the possibility of anomalous scaling we use a straightforward generalisation of the diffusive scaling function, with arbitrary exponent α ,

$$\mathcal{C}(x, t) = \frac{\kappa}{(Dt)^\alpha} \exp \left[- \left(\frac{x}{(Dt)^\alpha} \right)^2 \right], \quad (7)$$

where the factors κ and D may depend only on temperature. Assuming this scaling, we extract the exponent by fitting a Gaussian to $\mathcal{C}(x, t)$ at fixed t , and then fitting the inverse-widths to a power-law,

$$W(t)^{-1} = (Dt)^{-\alpha}. \quad (8)$$

We also consider the possibility of KPZ scaling. Whilst there is no elementary form for this function, it is tabulated in [60]. This corresponds to a scaling exponent of

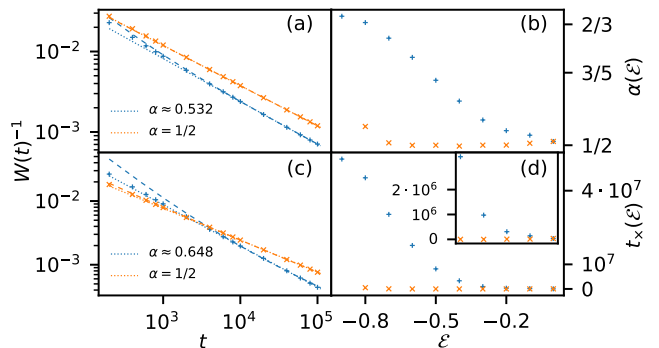


FIG. 1. Anomalous hydrodynamics in the FM: power-law scaling of the inverse-width of $\mathcal{C}^S(x, t)$, and extracted exponents and crossover scales for the FM (blue, +) and AFM (orange, \times). Panels (a) & (c) show $W(t)^{-1}$ for $\mathcal{E} = -0.3$ & $\mathcal{E} = -0.7$, resp. The dotted lines show the power-law fit (8), and the dashed lines show the finite-time corrected fit (9). Panel (b) shows the estimated anomalous exponents, assuming the scaling (7), whilst (d) shows the diffusion crossover times estimated from (9) – the inset zooms in on the points $\mathcal{E} = -0.4$ to $\mathcal{E} = 0$.

$\alpha_{\text{KPZ}} = 2/3$, and appears, e.g., in the spin correlations of the integrable $S = 1/2$ Heisenberg chain [8, 12].

Even when the long-time behaviour is diffusive, corrections are to be expected. For the classical $SU(2)$ spin chain, the lowest-order correction is $O(\sqrt{t})$ [53], and we therefore also fit the inverse-widths to a combination of power-laws,

$$W(t)^{-1} = (Dt)^{-1/2} + \Lambda t^{-1}. \quad (9)$$

When finite-time observations, either numerical or experimental, display apparently anomalous or KPZ-like behaviour, such a combination might be a plausible alternative interpretation [1, 53].

Equilibrium Correlations.— We show in Fig. 1(a) and 1(c) the widths of $\mathcal{C}^S(x, t)$ for the FM and AFM as a function of time at $\mathcal{E} = -0.3$ and $\mathcal{E} = -0.7$, for times $t = 200$ to $t = 10^5$.

The AFM displays ordinary spin diffusion, with the widths collapsing to the diffusive power-law after a comparatively short time $t \approx 10^3$. The FM does not exhibit diffusion, at any finite temperature, over the timescales of our simulations. Both (8) and (9) provide equally good two-parameter fits at long times.

If we interpret the observed lack of diffusion as evidence for superdiffusive scaling, the temperature dependence of the anomalous exponent is shown in Fig. 1(b). If, instead, we assume that we have a finite-time crossover, we may define an effective exponent via

$$\alpha_{\text{eff}}(t) = \frac{d \log(W)}{d \log(t)}, \quad (10)$$

and extract from (9) a crossover time t_\times defined, arbitrarily, by $\alpha_{\text{eff}}(t_\times) = 0.505$. The resulting crossover times are

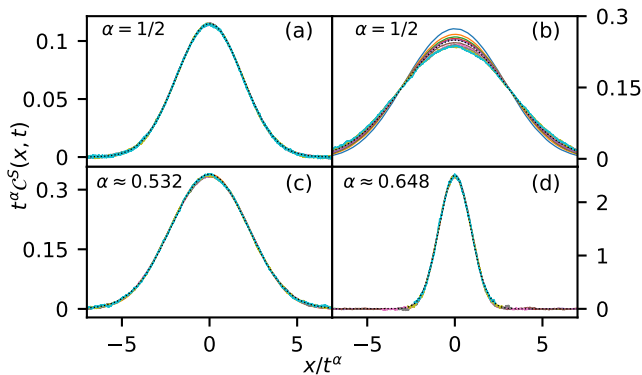


FIG. 2. Scaling collapses of the spin correlations $\mathcal{C}^S(x, t)$, with the scaling function (7). Colours correspond to different fixed times from $t = 2000$ to $t = 10^5$. Panel (a) shows the diffusive collapse at $\mathcal{E} = -0.3$ in the AFM; (b) shows the failure of the diffusive collapse at $\mathcal{E} = -0.3$ in the FM. Panels (c) and (d) show anomalous collapses at $\mathcal{E} = -0.3$ and $\mathcal{E} = -0.7$ in the FM, with exponents $\alpha = 0.532$ and $\alpha = 0.648$, resp.

shown in Fig. 1(d). Both Figs. 1(b) & 1(d) show a remarkable difference in behaviour between the FM and AFM models.

In Fig. 2 we show the scaling collapses at these temperatures. The AFM is clearly consistent with a diffusive collapse; the FM is not. A collapse with an anomalous exponent provides a much better fit to the ferromagnetic correlations, indicating anomalous scaling. However, we cannot exclude the possibility of a crossover – especially since the crossover times estimated from (9) are much larger than the timescales of the simulations.

KPZ Scaling.—We briefly remark on the evidence for KPZ scaling at low temperature in the FM, shown in Fig. 3. We find that the inverse-widths at $\mathcal{E} = -0.8$ fit almost perfectly to the power-law (8) with the KPZ exponent, $\alpha_{\text{KPZ}} = 2/3$, for three orders of magnitude in time. In isolation, the numerical evidence for KPZ scaling at $\mathcal{E} = -0.8$ is remarkably strong. Whilst it is not surprising that a drifting exponent would pass through $\alpha_{\text{KPZ}} = 2/3$, it is striking that all finite-time corrections apparently vanish exactly at this KPZ value. This tempts us to conclude that the model is in the KPZ universality class here; but the fact that this holds only over a narrow temperature range warrants caution.

Perhaps unsurprisingly, the KPZ scaling is less compelling at the lower energy of $\mathcal{E} = -0.9$ ($T = 0.1$), cf. Fig. 3(c). Indeed, at the lowest temperatures a (short-time) ballistic regime emerges, due to the increased spin-wave lifetime [58, 61]. This will affect the observed scaling on increasingly longer timescales.

Equilibration Dynamics.—In addition to our equilibrium simulations examining unequal-time correlations, we perform equilibration simulations probing the relaxation to thermal equilibrium after a quench. This allows us to test whether the anomalous behaviour or ultra-

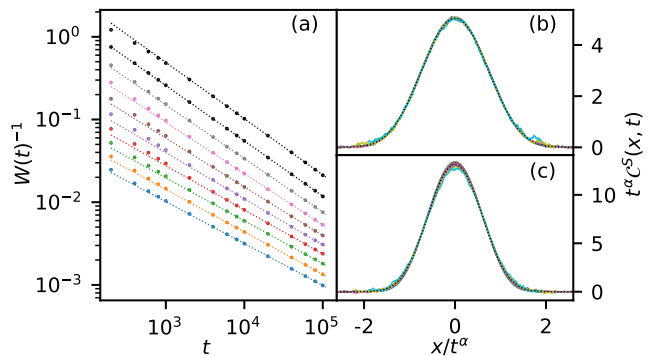


FIG. 3. Anomalous scaling in the FM. Panel (a) shows the inverse-widths, vertically offset for clarity, for, in descending order, $\mathcal{E} = -0.9$ to $\mathcal{E} = 0$ in steps of 0.1. The power-law fits have the exponents of Fig. 1b, except the black lines at $\mathcal{E} = -0.8$ and $\mathcal{E} = -0.9$, which are fit with the KPZ exponent $\alpha_{\text{KPZ}} = 2/3$. Panels (b) and (c) show the KPZ scaling collapse at $\mathcal{E} = -0.8$ and $\mathcal{E} = -0.9$, resp.

long-time crossover, and the distinction between FM and AFM, are also present in out-of-equilibrium dynamics.

We initially prepare the system in a thermal state of the XY chain,

$$\mathcal{H}_{\text{XY}} = -J \sum_{i=1}^L \mathbf{S}_i \cdot \mathbf{S}_{i+1} = -J \sum_{i=1}^L \cos(\phi_i - \phi_{i+1}), \quad (11)$$

for unit length classical rotors $\mathbf{S}_i \in S^1$. At time $t = 0$, we quench the system, and evolve under the dynamics (2) of the Heisenberg chain. We examine the relaxation of the following observables:

$$E^\mu(t) = -J \langle S_i^\mu(t) S_{i+1}^\mu(t) \rangle, \quad (12)$$

which measures the energy attributed to the μ^{th} spin components; and

$$Q^\mu(t) = \langle S_i^\mu(t)^2 \rangle, \quad (13)$$

which measures the total magnitude of the μ^{th} spin components. These are natural measures of the anisotropy, which characterises the relaxation from the initial state, satisfying $S_i^z = 0 \forall i$, to a (quasi-)thermal state of the isotropic Heisenberg chain. The equilibration of the energy fluctuations is measured using the heat capacity,

$$C(t) = \frac{\langle \text{var } E_i(t) \rangle}{T^2}, \quad (14)$$

where we take the spatial variance before the ensemble average to obtain a time-dependent quantity. As in the equilibrium simulations, we average over an ensemble of 20,000 states, initially drawn from the canonical ensemble of \mathcal{H}_{XY} .

We expect that the equilibration dynamics will be similarly hydrodynamic, since the relaxation to the new

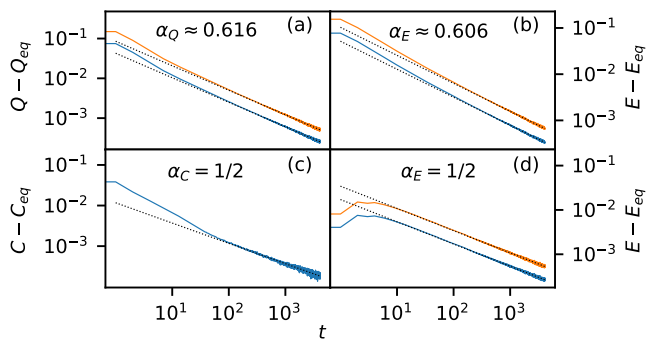


FIG. 4. Equilibration dynamics of $\mathcal{O}^z(t) - \mathcal{O}_{\text{eq}}^z$ (blue) and $\mathcal{O}^{\parallel}(t) - \mathcal{O}_{\text{eq}}^{\parallel}$ (orange), where $\mathcal{O}^{\parallel} = (\mathcal{O}^x + \mathcal{O}^y)/2$ is the average of the in-plane components. Panels (a), (b), and (c) show the equilibration of Q , E , and C at $\mathcal{E} = -0.5$ in the FM; (d) shows the equilibration of E at $\mathcal{E} = -0.5$ in the AFM. Q and E appear to equilibrate with an anomalous exponent of $\alpha \approx 0.6$ in the FM, though the data is equally well described by a combination of power-laws. The energy fluctuations (heat capacity) and the AFM equilibrate diffusively.

global equilibrium requires the transport of conserved densities over long distances [1]. The relaxation of an observable \mathcal{O} is therefore expected to follow a power-law

$$\delta\mathcal{O}(t) := |\mathcal{O}(t) - \mathcal{O}_{\text{eq}}| = \lambda t^{-\alpha}, \quad (15)$$

valid on some long timescale, where \mathcal{O}_{eq} is the thermal value of the observable in the Heisenberg chain.

These simulations exhibit complementary aspects of the same broad phenomenology observed in equilibrium. Fig. 4 shows the equilibration dynamics at $\mathcal{E} = -0.5$. The extracted (anomalous) equilibration exponents have qualitatively similar dependence on energy as those extracted from equilibrium correlation functions [58]. The energy fluctuations, as measured by the heat capacity, always equilibrate diffusively. In the AFM, E^μ and Q^μ also show diffusive equilibration. In the FM, however, the equilibration of E^μ and Q^μ is anomalous. Although E^μ is an energy, it is tied to the spin anisotropy, and therefore equilibrates anomalously in the FM, rather than tracking the diffusive behaviour of the energy fluctuations.

Thus, as in equilibrium, we observe a striking difference between the FM and AFM, with only the former displaying anomalous exponents. Whilst our simulations do not allow us to rule out a potential crossover to diffusive scaling at even longer times, the observables can reasonably be described to have (fully) equilibrated with these anomalous exponents, in particular when considering a realistic experimental situation in which resolution and time scales might be limited.

Discussion & Conclusions.—In summary, we have conducted a detailed numerical study of the equilibrium and out-of-equilibrium dynamics of the classical Heisenberg chain, with the largest system sizes, simulation times,

and range of temperatures we are aware of so far for this model.

Starting from the high-temperature paramagnetic regime we observe strong numerical evidence for ordinary diffusion of both spin and energy at $T = \infty$. In contrast, at intermediate temperatures the spin correlations of the FM depart from diffusion and display anomalous scaling over the accessible timescales in our simulations.

Thus, our study exposes a distinction, despite their identical thermodynamics, between the dynamics of the classical FM and AFM *even when the correlation length (5) is short*. Indeed, at $\mathcal{E} = -0.3$, where it is less than a single lattice spacing, one already observes a clear difference between the FM and AFM in Figs. 1 & 2.

The central open question thence concerns the origin of the vastly distinct scales and long-time dynamics. Whilst there is an obvious difference in that the order parameter of the FM (the magnetisation) is conserved, whereas the staggered magnetisation in the AFM is not [58], it is unclear why this should have such strong consequences when all correlations are short ranged and weak.

At low temperatures, we observe remarkably clean KPZ-like behaviour, in particular scaling with exponent $\alpha_{\text{KPZ}} = 2/3$ in the FM spin correlations. However, this is in evidence over a narrow temperature range only, and in addition non-abelian hydrodynamics [53] would seem to preclude KPZ scaling asymptotically. It is nonetheless intriguing that it is precisely in this apparent KPZ regime that finite-time corrections appear to be the weakest, and hence the anomalous scaling appears most reliable. In a different context, the numerical evidence for KPZ scaling would thus have seemed quite compelling.

Finally, we note that even if the apparently anomalous regimes eventually cross over to diffusion, their existence over extremely large intermediate scales is of obvious experimental importance, as coherent dynamics on the length- and timescales we have been able to probe in this study will not be straightforwardly accessible in most experimental platforms.

Acknowledgements: AMcR wishes to thank J. N. Hallen, and P. Suchsland for helpful discussions, and particularly B. A. Placke for explaining various aspects of C+++. This work was in part supported by the Deutsche Forschungsgemeinschaft under grants SFB 1143 (project-id 247310070) and the cluster of excellence ct.qmat (EXC 2147, project-id 390858490).

-
- [1] J. Lux, J. Müller, A. Mitra, and A. Rosch, Hydrodynamic long-time tails after a quantum quench, *Phys. Rev. A* **89**, 053608 (2014).
 [2] E. Leviatan, F. Pollmann, J. H. Bardarson, D. A. Huse, and E. Altman, Quantum thermalization dynamics with matrix-product states, *arXiv preprint arXiv:1702.08894* (2017).

- [3] M. Ljubotina, M. Žnidarič, and T. Prosen, Spin diffusion from an inhomogeneous quench in an integrable system, *Nature Communications* **8**, 16117 (2017).
- [4] M. Ljubotina, M. Žnidarič, and T. Prosen, Kardar-Parisi-Zhang physics in the quantum heisenberg magnet, *Phys. Rev. Lett.* **122**, 210602 (2019).
- [5] S. Gopalakrishnan and R. Vasseur, Kinetic theory of spin diffusion and superdiffusion in XXZ spin chains, *Phys. Rev. Lett.* **122**, 127202 (2019).
- [6] F. Weiner, P. Schmitteckert, S. Bera, and F. Evers, High-temperature spin dynamics in the heisenberg chain: Magnon propagation and emerging kardar-parisi-zhang scaling in the zero-magnetization limit, *Phys. Rev. B* **101**, 045115 (2020).
- [7] M. Fava, B. Ware, S. Gopalakrishnan, R. Vasseur, and S. A. Parameswaran, Spin crossovers and superdiffusion in the one-dimensional hubbard model, *Phys. Rev. B* **102**, 115121 (2020).
- [8] M. Dupont and J. E. Moore, Universal spin dynamics in infinite-temperature one-dimensional quantum magnets, *Phys. Rev. B* **101**, 121106 (2020).
- [9] V. B. Bulchandani, C. Karrasch, and J. E. Moore, Superdiffusive transport of energy in one-dimensional metals, *Proceedings of the National Academy of Sciences* **117**, 12713 (2020).
- [10] D. Schubert, J. Richter, F. Jin, K. Michielsen, H. De Raedt, and R. Steinigeweg, Quantum versus classical dynamics in spin models: chains, ladders, and planes, *arXiv:2104.00472* (2021).
- [11] J. Richter and A. Pal, *Anomalous hydrodynamics in a class of scarred frustration-free hamiltonians* (2021), *arXiv:2107.13612* [cond-mat.stat-mech].
- [12] M. Dupont, N. E. Sherman, and J. E. Moore, *Spatiotemporal crossover between low- and high-temperature dynamical regimes in the quantum heisenberg magnet* (2021), *arXiv:2104.13393* [cond-mat.str-el].
- [13] A. Gromov, A. Lucas, and R. M. Nandkishore, Fracton hydrodynamics, *Phys. Rev. Research* **2**, 033124 (2020).
- [14] J. Feldmeier, P. Sala, G. De Tomasi, F. Pollmann, and M. Knap, Anomalous diffusion in dipole- and higher-moment-conserving systems, *Phys. Rev. Lett.* **125**, 245303 (2020).
- [15] A. Morningstar, V. Khemani, and D. A. Huse, Kinetically constrained freezing transition in a dipole-conserving system, *Phys. Rev. B* **101**, 214205 (2020).
- [16] D. Bernard and B. Doyon, Conformal field theory out of equilibrium: a review, *Journal of Statistical Mechanics: Theory and Experiment* **2016**, 064005 (2016).
- [17] O. A. Castro-Alvaredo, B. Doyon, and T. Yoshimura, Emergent hydrodynamics in integrable quantum systems out of equilibrium, *Phys. Rev. X* **6**, 041065 (2016).
- [18] B. Bertini, M. Collura, J. De Nardis, and M. Fagotti, Transport in out-of-equilibrium XXZ chains: exact profiles of charges and currents, *Phys. Rev. Lett.* **117**, 207201 (2016).
- [19] V. B. Bulchandani, R. Vasseur, C. Karrasch, and J. E. Moore, Solvable hydrodynamics of quantum integrable systems, *Physical review letters* **119**, 220604 (2017).
- [20] S. Sotiriadis, Equilibration in one-dimensional quantum hydrodynamic systems, *Journal of Physics A: Mathematical and Theoretical* **50**, 424004 (2017).
- [21] E. Ilievski and J. De Nardis, Microscopic origin of ideal conductivity in integrable quantum models, *Phys. Rev. Lett.* **119**, 020602 (2017).
- [22] B. Doyon, H. Spohn, and T. Yoshimura, A geometric viewpoint on generalized hydrodynamics, *Nuclear Physics B* **926**, 570–583 (2018).
- [23] B. Doyon, T. Yoshimura, and J.-S. Caux, Soliton gases and generalized hydrodynamics, *Physical review letters* **120**, 045301 (2018).
- [24] V. B. Bulchandani, R. Vasseur, C. Karrasch, and J. E. Moore, Bethe-boltzmann hydrodynamics and spin transport in the XXZ chain, *Physical Review B* **97**, 045407 (2018).
- [25] B. Doyon, Lecture notes on generalised hydrodynamics, *arXiv preprint arXiv:1912.08496* (2019).
- [26] P. Ruggiero, P. Calabrese, B. Doyon, and J. Dubail, Quantum generalized hydrodynamics, *Phys. Rev. Lett.* **124**, 140603 (2020).
- [27] J. Dufty, K. Luo, and J. Wrighton, Generalized hydrodynamics revisited, *Phys. Rev. Research* **2**, 023036 (2020).
- [28] V. Alba, B. Bertini, M. Fagotti, L. Piroli, and P. Ruggiero, Generalized-hydrodynamic approach to inhomogeneous quenches: correlations, entanglement and quantum effects (2021), *arXiv:2104.00656* [cond-mat.stat-mech].
- [29] A. J. Friedman, S. Gopalakrishnan, and R. Vasseur, Diffusive hydrodynamics from integrability breaking, *Phys. Rev. B* **101**, 180302 (2020).
- [30] J. Lopez-Piqueres, B. Ware, S. Gopalakrishnan, and R. Vasseur, Hydrodynamics of nonintegrable systems from a relaxation-time approximation, *Phys. Rev. B* **103**, L060302 (2021).
- [31] M. Kardar, G. Parisi, and Y.-C. Zhang, Dynamic scaling of growing interfaces, *Phys. Rev. Lett.* **56**, 889 (1986).
- [32] H. Spohn, Exact solutions for KPZ-type growth processes, random matrices, and equilibrium shapes of crystals, *Physica A: Statistical Mechanics and its Applications* **369**, 71–99 (2006).
- [33] T. Sasamoto and H. Spohn, Exact height distributions for the KPZ equation with narrow wedge initial condition, *Nuclear Physics B* **834**, 523–542 (2010).
- [34] G. Amir, I. Corwin, and J. Quastel, Probability distribution of the free energy of the continuum directed random polymer in $1 + 1$ dimensions, *Communications on Pure and Applied Mathematics* **64**, 466–537 (2010).
- [35] T. Kriecherbauer and J. Krug, A pedestrian's view on interacting particle systems, KPZ universality and random matrices, *Journal of Physics A: Mathematical and Theoretical* **43**, 403001 (2010).
- [36] J. Quastel and H. Spohn, The one-dimensional KPZ equation and its universality class, *Journal of Statistical Physics* **160**, 965–984 (2015).
- [37] H. van Beijeren, Exact results for anomalous transport in one-dimensional hamiltonian systems, *Phys. Rev. Lett.* **108**, 180601 (2012).
- [38] M. Kulkarni and A. Lamacraft, Finite-temperature dynamical structure factor of the one-dimensional bose gas: From the gross-pitaevskii equation to the kardar-parisi-zhang universality class of dynamical critical phenomena, *Phys. Rev. A* **88**, 021603 (2013).
- [39] S. G. Das, A. Dhar, K. Saito, C. B. Mendl, and H. Spohn, Numerical test of hydrodynamic fluctuation theory in the fermi-pasta-ulam chain, *Phys. Rev. E* **90**, 012124 (2014).
- [40] H. Spohn, Nonlinear fluctuating hydrodynamics for anharmonic chains, *Journal of Statistical Physics* **154**, 1191 (2014).
- [41] C. B. Mendl and H. Spohn, Equilibrium time-correlation functions for one-dimensional hard-point systems, *Phys.*

- Rev. E **90**, 012147 (2014).
- [42] M. Kulkarni, D. A. Huse, and H. Spohn, Fluctuating hydrodynamics for a discrete gross-pitaevskii equation: Mapping onto the kardar-parisi-zhang universality class, *Phys. Rev. A* **92**, 043612 (2015).
- [43] C. B. Mendl and H. Spohn, Searching for the Tracy-Widom distribution in nonequilibrium processes, *Phys. Rev. E* **93**, 060101 (2016).
- [44] Z. Chen, J. de Gier, I. Hiki, and T. Sasamoto, Exact confirmation of 1d nonlinear fluctuating hydrodynamics for a two-species exclusion process, *Phys. Rev. Lett.* **120**, 240601 (2018).
- [45] S. Lepri, R. Livi, and A. Politi, Too close to integrable: crossover from normal to anomalous heat diffusion, *Phys. Rev. Lett.* **125**, 040604 (2020).
- [46] A. Das, M. Kulkarni, H. Spohn, and A. Dhar, Kardar-parisi-zhang scaling for an integrable lattice Landau-Lifshitz spin chain, *Phys. Rev. E* **100**, 042116 (2019).
- [47] R. W. Gerling and D. P. Landau, Comment on “anomalous spin diffusion in classical Heisenberg magnets”, *Phys. Rev. Lett.* **63**, 812 (1989).
- [48] R. Gerling and D. Landau, Time-dependent behavior of classical spin chains at infinite temperature, *Physical Review B* **42**, 8214 (1990).
- [49] M. Böhm, R. W. Gerling, and H. Leschke, Comment on “breakdown of hydrodynamics in the classical 1d Heisenberg model”, *Physical review letters* **70**, 248 (1993).
- [50] N. Srivastava, J.-M. Liu, V. Viswanath, and G. Müller, Spin diffusion in classical Heisenberg magnets with uniform, alternating, and random exchange, *Journal of Applied Physics* **75**, 6751 (1994).
- [51] V. Oganesyan, A. Pal, and D. A. Huse, Energy transport in disordered classical spin chains, *Physical Review B* **80**, 115104 (2009).
- [52] D. Bagchi, Spin diffusion in the one-dimensional classical Heisenberg model, *Physical Review B* **87**, 075133 (2013).
- [53] P. Glorioso, L. V. Delacrétaz, X. Chen, R. M. Nandkishore, and A. Lucas, Hydrodynamics in lattice models with continuous non-Abelian symmetries, *SciPost Phys.* **10**, 15 (2021).
- [54] G. Müller, Anomalous spin diffusion in classical Heisenberg magnets, *Physical review letters* **60**, 2785 (1988).
- [55] O. de Alcantara Bonfim and G. Reiter, Breakdown of hydrodynamics in the classical 1d Heisenberg model, *Physical review letters* **69**, 367 (1992).
- [56] O. de Alcantara Bonfim and G. Reiter, de Alcantara Bonfim and Reiter reply, *Physical review letters* **70**, 249 (1993).
- [57] J. De Nardis, M. Medenjak, C. Karrasch, and E. Ilievski, Universality classes of spin transport in one-dimensional isotropic magnets: The onset of logarithmic anomalies, *Physical Review Letters* **124**, 210605 (2020).
- [58] See Supplementary Material at [URL will be inserted by publisher] for additional details on the exact thermodynamics, the numerical methods, including the construction of thermal states and time-evolution, results on the infinite temperature case, the energy correlations, staggered magnetisation, and the equilibration dynamics and extracted equilibration exponents.
- [59] M. E. Fisher, Magnetism in one-dimensional systems—the Heisenberg model for infinite spin, *American Journal of Physics* **32**, 343 (1964).
- [60] M. Prähofer and H. Spohn, Exact scaling functions for one-dimensional stationary KPZ growth, *Journal of statistical physics* **115**, 255 (2004).
- [61] T. Bilitewski, S. Bhattacharjee, and R. Moessner, Classical many-body chaos with and without quasiparticles, *Phys. Rev. B* **103**, 174302 (2021).
- [62] D. Loison, C. Qin, K. Schotte, and X. Jin, Canonical local algorithms for spin systems: heat bath and Hastings’s methods, *The European Physical Journal B-Condensed Matter and Complex Systems* **41**, 395 (2004).

Supplementary Material

CONTENTS

In this supplementary we provide further details of our simulations, and further evidence for our conclusions. In S-I we provide the exact thermodynamics of the XY and Heisenberg chains. S-II contains an account of our numerical methods for the construction of thermal states and time evolution. In S-III we show evidence for spin diffusion at infinite temperature, and in S-IV we show the diffusion of energy at all temperatures.

In S-V we examine the staggered correlations – i.e. the correlations of the AFM order parameter. Finally, in S-VI we provide more information about our equilibration simulations, and provide the extracted anomalous exponents.

S-I. EXACT THERMODYNAMICS

For reference, we provide here the exact thermodynamics of the classical Heisenberg [59] and XY chains. The derivation is given with open boundary conditions, since this is simpler - but the boundary effects vanish in the thermodynamic limit.

Consider first the XY chain. The partition function is

$$\begin{aligned} Z_{XY} &= \int \left(\prod_{i=1}^N \frac{d\phi_i}{2\pi} \right) \exp(\beta J \sum_{i=1}^{N-1} \cos(\phi_i - \phi_{i+1})) \\ &= \prod_{i=1}^{N-1} \int \frac{d\varphi_i}{2\pi} \exp(\beta J \cos(\varphi_i)) \times \int \frac{d\varphi_N}{2\pi} \\ &= I_0(\beta J)^{N-1}, \end{aligned} \quad (\text{S1})$$

where I_n denotes a modified Bessel function of the first kind, and in the second line we have transformed the coordinates to $\varphi_i = \phi_i - \phi_{i+1}$. Similarly, the partition function of the Heisenberg chain is

$$\begin{aligned} Z &= \int \left(\prod_{i=1}^N \frac{d\mathbf{S}_i}{4\pi} \right) \exp(\beta J \sum_{i=1}^{N-1} \mathbf{S}_i \cdot \mathbf{S}_{i+1}) \\ &= \int \frac{d\hat{\Omega}_1}{4\pi} \times \prod_{i=2}^N \int \frac{d\hat{\Omega}_i}{4\pi} \exp(\beta J \cos(\theta_i)) \\ &= \left(\frac{\sinh(\beta J)}{\beta J} \right)^{N-1}, \end{aligned} \quad (\text{S2})$$

where, in the second line, we rotate the coordinate system of \mathbf{S}_{i+1} such that the z -axis aligns with \mathbf{S}_i .

From these expressions, all of the thermodynamic quantities may be calculated. In particular, taking the

thermodynamic limit and setting $J = 1$, the internal energy density and specific heat are:

$$\begin{aligned} \mathcal{E}_{XY}(T) &= -I_1(1/T)/I_0(1/T), \\ C_{XY}(T) &= \frac{1}{T^2} \left(\frac{I_2(1/T) + I_0(1/T)}{2I_0(1/T)} - \frac{I_1(1/T)^2}{I_0(1/T)^2} \right) \end{aligned} \quad (\text{S3})$$

for the XY chain, and:

$$\begin{aligned} \mathcal{E}(T) &= T - \coth(1/T), \\ C(T) &= 1 - \frac{\text{csch}(1/T)^2}{T^2} \end{aligned} \quad (\text{S4})$$

for the Heisenberg chain. The equal-time two-point correlation function is given by

$$\langle \mathbf{S}_i \cdot \mathbf{S}_j \rangle = (-\mathcal{E})^{|i-j|} =: e^{-|i-j|/\xi}, \quad (\text{S5})$$

and so the correlation length is

$$\xi(\mathcal{E}) = -1/\log(-\mathcal{E}), \quad (\text{S6})$$

which, as a function of internal energy, is the same for both the XY and Heisenberg chains. In the antiferromagnet, the above is replaced with the staggered correlator.

S-II. NUMERICAL METHODS

A. Construction of Thermal States

Our initial thermal states are constructed using a heat-bath Monte Carlo method [62], where we use the fact that we can precisely invert the thermal probability distribution for a single spin in a magnetic field.

The general method is known as inverse transform sampling. Let $X \in [a, b] \subseteq \mathbb{R}$ a random variable on some real interval, with probability distribution $p(X)$. The cumulative distribution function (CDF) is

$$\mathcal{F}_X(x) = \int_a^x dX p(X), \quad (\text{S7})$$

i.e., the probability that a randomly sampled X is less than or equal to x . Then the random variable $Y = \mathcal{F}_X^{-1}(u)$, where u is uniformly random over $[0, 1]$, has the same probability distribution as the original variable X since, by construction,

$$\mathcal{F}_Y(x) = \int_0^{u=\mathcal{F}_X(x)} du' = \mathcal{F}_X(x). \quad (\text{S8})$$

The specific problem is to invert the CDF. For a Heisenberg spin, this can be done analytically. Letting $\mathbf{h} = h\hat{z}$, the CDF for S^z is

$$\mathcal{F}_z(S^z) = \int_{-1}^{S^z} dz \frac{e^{\beta h z}}{\mathcal{Z}} = \frac{\int_{-1}^{S^z} dz e^{\beta h z}}{\int_{-1}^1 dz e^{\beta h z}} = \frac{e^{\beta h S^z} - e^{-\beta h}}{e^{\beta h} - e^{-\beta h}}. \quad (\text{S9})$$

Then, using $\mathcal{F}_z(\mathcal{F}_z^{-1}(u)) = u$, we find that we can sample S^z as

$$S^z = \mathcal{F}_z^{-1}(u) = 1 + \frac{\log(1 - u + ue^{-2\beta h})}{\beta h}. \quad (\text{S10})$$

The S^x and S^y components have random direction in the plane, and magnitude set by the condition $|\mathbf{S}| = 1$. For a magnetic field of arbitrary direction, one need only appropriately rotate the sampled spin.

For XY spins, the inversion cannot be performed analytically. In this case, we let $\mathbf{h} = h\hat{\mathbf{x}}$, and sample the angle ϕ , where $(S^x, S^y) = (\cos(\phi), \sin(\phi))$, by numerically solving the integral equation

$$u = \int_{-\pi}^{\phi} d\phi' \frac{e^{\beta h \cos(\phi')}}{I_0(\beta h)}, \quad (\text{S11})$$

for randomly generated u . Again, the generalisation to arbitrary magnetic field direction is via a rotation.

To sample a state from the canonical ensemble, we randomly generate the first spin \mathbf{S}_1 . We then sweep through the chain, generating \mathbf{S}_{i+1} from the thermal distribution of the effective field $\mathbf{h} = J\mathbf{S}_i$. For open boundary conditions, cf. the coordinate transformations used to calculate the partition functions, this exactly samples the canonical ensemble. For periodic boundary conditions we perform an additional 1000 sweeps through the chain.

B. Time Evolution

For the equilibration simulations, we integrate the equations of motion with the standard fourth-order Runge-Kutta (RK4) method, using a fixed timestep of $\Delta t = 0.002J^{-1}$. This method conserves the magnetisation to machine precision, and for a system size $L = 16384$ and a final time $t_f = 4096J^{-1}$ the error in the energy density is limited to $\sim 10^{-10}$.

For the equilibrium simulations, we use a system size of $L = 8192$, but a much longer final time $t_f = 1.1 \times 10^5 J^{-1}$. To achieve such times, we use the discrete-time odd-even (DTOE) method, with a larger timestep of $\Delta t = 0.05J^{-1}$. The method consists of updating the odd spins for a timestep Δt by exactly solving the equations of motion with the even spins held fixed, and then vice versa. This method conserves the energy to machine precision, but the error in the magnetisation is suppressed only as $O(\Delta t^2)$. However, this algorithm is symplectic, and thus the error does not grow with time – for the timestep chosen the magnetisation error is $\sim 10^{-5}$.

S-III. SPIN DIFFUSION AT INFINITE TEMPERATURE

There has been some recent controversy over the nature of the hydrodynamics at $T = \infty$ in the Heisenberg

chain, with [57] claiming logarithmically enhanced diffusion and [53] arguing for ordinary spin diffusion. Here we provide our own contribution to this debate: we see no evidence for logarithmically enhanced diffusion.

In Fig. S1 we show, for $T = \infty$, the inverse-widths fit to the diffusive power-law, and the scaling collapse of the spin correlations from $t = 2000$ to $t = 10^5$. Note that the ferromagnet and antiferromagnet are indistinguishable at infinite temperature.

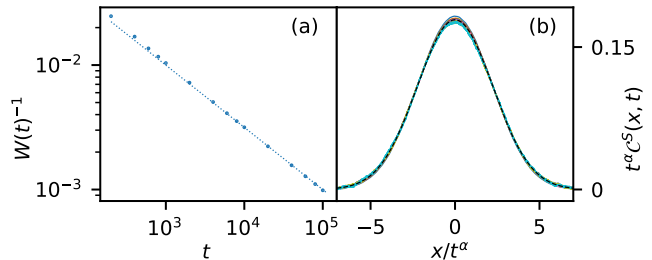


FIG. S1. Spin diffusion at infinite temperature. Panel (a) shows the fit to the power-law with $\alpha = 1/2$; panel (b) shows the scaling collapse.

S-IV. ENERGY CORRELATIONS

We have reported in the main text that the energy correlations are found to be diffusive for both the FM and the AFM. We show the evidence for this in Fig. S2, where we plot the Gaussian width of the energy correlations $\mathcal{C}^E(x, t)$ as a function of time. We find that, except at the lowest temperatures, they are well-fit by the diffusive power-law.

At low temperatures, ballistically propagating spin-wave modes persist to intermediate times. This makes

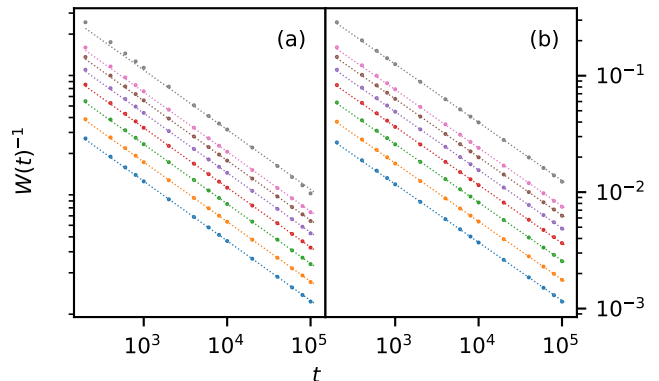


FIG. S2. Energy diffusion in (a) the FM and (b) the AFM. The inverse-widths of $\mathcal{C}^E(x, t)$ with the fit to the diffusive power-law are plotted, in ascending order, for $\mathcal{E} = 0$ to $\mathcal{E} = -0.7$, in steps of -0.1 . The data are shifted vertically for clarity.

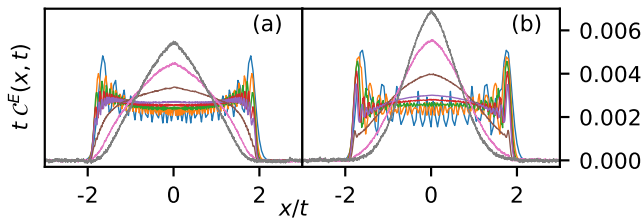


FIG. S3. Short time ballistic propagation of the energy correlations at low temperature, $\mathcal{E} = -0.9$ ($T = 0.1$), for (a) the FM and (b) the AFM. The fixed times are: $t = 20$ (blue), $t = 40$ (orange), $t = 60$ (green), $t = 80$ (red), $t = 100$ (purple), $t = 200$ (brown), $t = 400$ (pink), and $t = 600$ (grey).

the observation of diffusion in our simulations rather difficult – even at longer times where the ballistic modes have decayed – because, over their lifetime, the ballistic modes increase the width of the correlations much faster than diffusion. By the time this effect is negligible, the width is comparable to the system size, and finite size effects take over. We show in Fig. S3 the ballistic collapse of the front.

S-V. DECAY OF STAGGERED CORRELATIONS

The most striking result of our study is the apparently different hydrodynamics of the ferromagnetic and antiferromagnetic chains, manifested in the spin correlations. We speculate in our discussion that this is related to the fact that the hydrodynamic mode, the magnetisation, is the order parameter of the FM but not the AFM – though precisely how this feeds into the scaling is not resolved.

The correlations of the staggered magnetisation are not conserved. Attempting to construct such a correlator, we find:

$$\begin{aligned} \mathcal{C}^A(i, t; j, t') &= \langle (-1)^i \mathbf{S}_i(t) \cdot (-1)^j \mathbf{S}_j(t') \rangle \\ &= (-1)^{i+j} \langle \mathbf{S}_i(t) \cdot \mathbf{S}_j(t') \rangle \\ &= (-1)^{i-j+2j} \langle \mathbf{S}_i(t) \cdot \mathbf{S}_j(t') \rangle \\ &= (-1)^{|i-j|} \langle \mathbf{S}_i(t) \cdot \mathbf{S}_j(t') \rangle, \end{aligned} \quad (\text{S12})$$

and so, writing $\mathcal{C}^A(i-j, t-t') = \mathcal{C}^A(i, t; j, t')$, we have

$$\mathcal{C}^A(j, t) = (-1)^j \mathcal{C}^S(j, t). \quad (\text{S13})$$

Now, $\mathcal{C}^S(j, t)$ is conserved in the sense that

$$\sum_j \mathcal{C}^S(j, t) = \sum_{j=-L/2}^{L/2-1} e^{-|j|/\xi} \quad (\text{S14})$$

is independent of time. The sum $\sum_j \mathcal{C}^A(j, t)$ is not similarly conserved, and its rapid decay with time is plotted in Fig. S4.

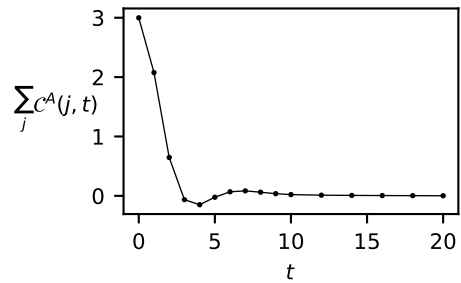


FIG. S4. Decay of the total staggered correlations as a function of time at $\mathcal{E} = -0.5$ in the antiferromagnet.

Note that this does *not* imply that the staggered order itself decays – in our equilibrium simulations, the system remains in a thermal state throughout, and thus, in expectation,

$$\mathcal{C}^A(i, t; j, t) = \mathcal{C}^A(i, 0; j, 0) = e^{-|i-j|/\xi}. \quad (\text{S15})$$

What is implied by the decay of $\sum_j \mathcal{C}^A(j, t)$ is that the staggered magnetisation at one time is uncorrelated with the staggered magnetisation at another. It therefore does not constitute a hydrodynamic mode, and it does not make sense to consider any scaling of this correlator.

S-VI. EQUILIBRATION DYNAMICS

We provide here some further details of the equilibration simulations – in particular, how we determine the thermal values, and the temperature dependence of the (finite-time) anomalous exponents.

We begin from a thermal state of the XY chain, with every spin confined to the plane $S^z = 0$, and evolve towards a quasi-thermal state of the Heisenberg chain. Recall from the main text that we measure the degree of anisotropy with the observables

$$E^\mu(t) = -J \langle S_i^\mu(t) S_{i+1}^\mu(t) \rangle \quad (\text{S16})$$

and

$$Q^\mu(t) = \langle S_i^\mu(t)^2 \rangle. \quad (\text{S17})$$

For a state with energy density \mathcal{E} , these observables are constrained by $\sum_\mu Q^\mu = 1$ and $\sum_\mu E^\mu = \mathcal{E}$. Their Heisenberg equilibrium values are thus determined by isotropy, to wit, $Q_{\text{eq}}^\mu = 1/3$ and $E_{\text{eq}}^\mu = \mathcal{E}/3$.

There is a caveat: at finite size there is a small, but conserved, total magnetisation, which prevents Q^μ and E^μ from attaining their precise equilibrium values. However, this correction may be calculated exactly. Given, at system size L , the $q = 0$ component of the static structure factor,

$$\Delta(L) = \frac{1}{L} \sum_{j=-L/2}^{L/2-1} (-\mathcal{E})^{|j|}, \quad (\text{S18})$$

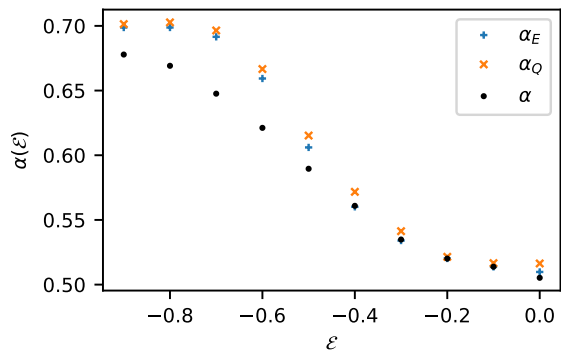


FIG. S5. Anomalous equilibration exponents α_E and α_Q for the observables E^μ and Q^μ in the FM. The measured equilibrium exponent is also shown for comparison. The discrepancy at low-temperature is probably due to timescales – the equilibrium exponent is extracted over the range $t = 10,000$ to $t = 100,000$, whereas the equilibration exponents are extracted up to $t = 4096$.

the asymptotic values are:

$$\begin{aligned} Q^z &\rightarrow 1/3 - \Delta/3, & Q^\parallel &\rightarrow 1/3 + \Delta/6, \\ E^z &\rightarrow \mathcal{E}/3 + J\Delta/3, & E^\parallel &\rightarrow \mathcal{E}/3 - J\Delta/6, \end{aligned} \quad (\text{S19})$$

where we have defined the averages of the in-plane observables, $Q^\parallel = (Q^x + Q^y)/2$ and $E^\parallel = (E^x + E^y)/2$. We take the average of the two in-plane components to account for the finite-size magnetisation spontaneously breaking the rotational symmetry of the initial XY state – which means we can read off the initial values exactly from the sum rules.

To examine the equilibration of energy fluctuations, we consider the heat capacity. Recall that the heat capacity can be estimated from a thermal ensemble as

$$C = \frac{\partial \langle E \rangle}{\partial T} = \frac{\langle E^2 \rangle - \langle E \rangle^2}{T^2}, \quad (\text{S20})$$

where E is the energy of the state and the angle brackets denote the *ensemble* average. Since the energy of each state is conserved by the Hamiltonian dynamics, this is time-independent.

However, we define the heat capacity of a *single state* as

$$C = \frac{\text{var } E_i}{T^2}, \quad (\text{S21})$$

where the variance is taken over the spatial distribution of the energy. In equilibrium, this is equal to the ensemble-based definition (S20), but it is not conserved by the dynamics. The initial value, of course, is the heat capacity (S3) of the XY chain, except that, since the correspondence between internal energy and temperature is different in the two chains, we must multiply the above by $(T_{XY}/T_H)^2$, with T_{XY} and T_H the temperatures that correspond to \mathcal{E} . The equilibrium value C_{eq} is then given by the heat capacity of the Heisenberg chain (S4).

As mentioned in the main text, the equilibration simulations probe a different aspect of the underlying phenomenology: Q^μ and E^μ equilibrate diffusively in the AFM, but anomalously in the FM. The heat capacity always equilibrates diffusively.

The anomalous exponents obtained from the equilibration in the FM are shown in Fig. S5.